

Numerical simulation of quenching of large sized blocks of 718 steel used for plastic dies

D.-L. Song, J.-F. Gu, J.-S. Pan and M.-J. Hu

The 718 steel used for plastic dies is required to be prehardened to 29–35HRC. For large sized blocks, it is relatively difficult to additionally guarantee uniform hardness with the greatest hardness difference of 3HRC and without any quenching cracks after heat treatment. In this paper, the transient temperature field and microstructure transformation during the quenching process of large sized blocks of 718 steel have been simulated numerically. Based on the simulation and experimental results, an appropriate quenching process, that is, direct air cooled quenching after austenitising at higher temperatures such as 880–930°C, was recommended in order to reach hardness uniformity and avoid quenching cracks. MST/5941

Keywords: Quenching, Numerical simulation, Hardness, 718 steel used for plastic die, Finite element method (FEM)

The authors are in the School of Material Science & Engineering, Staff Room 560, Shanghai Jiao Tong University, 1954 Huashan Road, Shanghai 200030, China (winter_song@sjtu.edu.cn). Manuscript received 14 August 2003; accepted 5 June 2004.

© 2004 Institute of Materials, Minerals and Mining. Published by Maney on behalf of the Institute.

Introduction

Quenching, during which workpieces are cooled at a fast rate from a higher temperature, is the most important operation of heat treatment. A bainite or martensite microstructure is expected to result after quenching. However, such results can not always be realised because of the complicated quenching involved, including the characteristics of the processed steels as well as the attributes of the quenchants. The physical nature of quenching is a constitutive model coupling the temperature, phase transformation and stress/strain in the processed parts. Recently, great progress has been achieved in quenching model research and computer simulation, such as in the coupling between temperature, phase transformation and stress,^{1–3} three dimensional nonlinear FEM analysis,^{4,5} the calculation of phase transformation kinetics,^{6–8} the effect of stress on phase transformation kinetics^{9–11} and dealing with an abruptly changed boundary condition.^{12,13} All these provide a sound basis for the application of computer simulation technology in manufacturing. In this paper, the temperature and microstructure fields of large sized blocks during quenching were simulated in terms of commercial finite element (FE) software MSC-Marc and user defined subroutines. By combining the experiment results, a suitable quenching process for large sized 718 steel blocks used for plastic die is proposed. This quenching process can guarantee uniform hardness without any quenching cracks.

Mathematical model and FEM numerical analysis

TRANSIENT TEMPERATURE FIELD

The transient temperature field during quenching can be described by the following partial differential equations.

$$\frac{\partial}{\partial x} \left(\lambda \frac{\partial T}{\partial x} \right) + \frac{\partial}{\partial y} \left(\lambda \frac{\partial T}{\partial y} \right) + \frac{\partial}{\partial z} \left(\lambda \frac{\partial T}{\partial z} \right) + \dot{q} = \rho c_p \frac{\partial T}{\partial \tau} \quad (1)$$

where λ , ρ and c_p are thermal conductivity, density and specific heat, and these thermophysical property parameters are strongly temperature dependent. \dot{q} , the internal heat

source as a result of the latent heat released during phase transformation, can be expressed as^{10,14}

$$\dot{q} = \frac{\Delta f \cdot \Delta H}{\Delta t} \quad (2)$$

where Δf and ΔH are the volume fraction and the enthalpy of new phase.

The boundary conditions can be divided into three kinds

$$\text{Boundary } s_1 : T_{s_1} = T_s(x, y, z, t) \quad (3)$$

$$\text{Boundary } s_2 : -k \left(\frac{\partial T}{\partial n} \right)_{s_2} = \dot{q}_s(x, y, z, t) \quad (4)$$

$$\text{Boundary } s_3 : -k \left(\frac{\partial T}{\partial n} \right)_{s_3} = h_\Sigma (T_s - T_a) \quad (5)$$

where $\partial T / \partial n$ is the temperature gradient on the boundary along external normal direction, \dot{q}_s is the heat density of the workpiece surface, T_s is the temperature of workpiece surface (°C), T_a is the temperature of the quenchants (°C) and h_Σ is the comprehensive heat transfer coefficient.

$$h_\Sigma = h_c + h_r \quad (6)$$

$$h_r = \varepsilon \sigma (T_a^2 + T_s^2)(T_a + T_s) \quad (7)$$

where, h_c and h_r are temperature dependent convective and radiant heat transfer coefficient, ε is the radiation emissivity of the workpiece, set as 0.6 in this paper and σ is the Stefan–Boltzmann constant with the value of $5.768 \times 10^{-8} \text{ W m}^{-2} \text{ K}^{-4}$.

In this paper, boundary s_3 is adopted as the boundary condition. When cooling in air, h_Σ can be calculated as the following

$$h_\Sigma = 2 \cdot 2(T_s + T_a)^{0.25} + 4 \cdot 6 \cdot 10^{-6}(T_a^2 + T_s^2)(T_a + T_s)^7$$

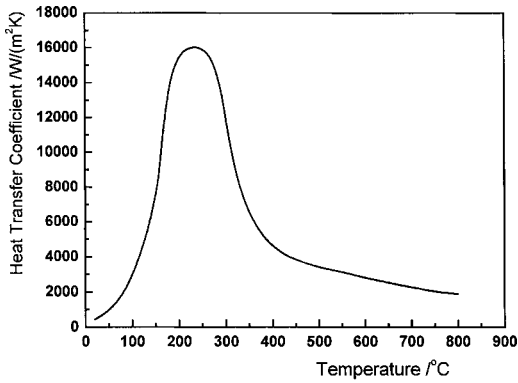
When cooling in water, h_Σ can be determined by means of the ‘inverse heat transfer method’ (IHTM), shown in Fig. 1.¹⁵

The initial condition is

$$T|_{t=0} = T_0(x, y, z) \quad (8)$$

The three dimensional FEM format of the temperature field equation can be deduced as^{4,16}

$$[\mathbf{K}]\{\mathbf{T}\}_t + [\mathbf{C}]\left\{\frac{\partial \mathbf{T}}{\partial t}\right\}_t = \{\mathbf{F}\}_t \quad (9)$$



1 Heat transfer coefficient of water

The backward difference method was used to discretise the time domain, so the following equation can be obtained.

$$\left([K] + \frac{1}{\Delta t} [C] \right) \{T\}_t = \frac{1}{\Delta t} [C] \{T\}_{t-\Delta t} + \{F\} \quad (10)$$

where [C] is the heat capacity matrix, [K] is the conductivity matrix. {F} is the vector of internal heat generation. The transient temperature field can be obtained by solving this large equation group.

PHASE TRANSFORMATION

To calculate the volume fraction of diffusion-type phase transformations during continuous cooling, the start times of phase transformation, that is, incubation period, need to be determined. The cooling path is divided into many segments that could be approximately treated as *iso*-temperature time intervals. The incubation period then can be calculated by applying an additivity rule.^{17,18}

$$\sum \frac{\Delta t_i}{\tau_i(T)} = 1 \quad \dots \quad (10)$$

where $\tau_i(T)$ is the incubation period of the TTT diagram at the temperature of T , Δt_i is the time interval held at a temperature of T . When the total incubation time reaches 1, the volume fraction of the new phase starts to be calculated by the Avrami equation.¹⁹

$$f = 1 - \exp(-bt^n) \quad \dots \quad (11)$$

When calculating the volume fraction of diffusion-type phase transformation, the virtual time was introduced. The virtual time, obtained by equation (12), is the time needed to form, at the temperature T_i , the volume fraction of the new phase equal to that transformed in a full spectrum of temperatures higher than T_i .

$$t_i^* = \left[-\frac{\ln(1-f_{i-1})}{b_i} \right]^{1/n_i} \quad \dots \quad (12)$$

If the temperature of T_i is kept for the time interval of Δt , the virtual volume fraction of the new phase is

$$f_i^* = 1 - \exp(-b_i(t_i^* + \Delta t)^n) \quad \dots \quad (13)$$

The real volume fraction is

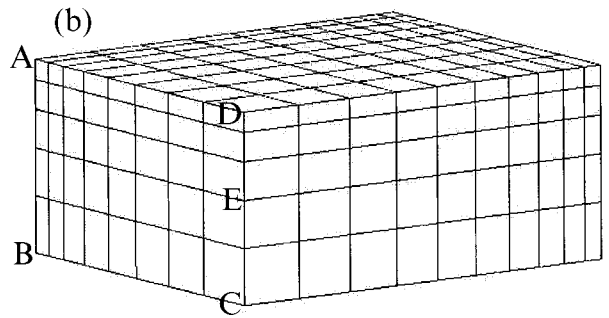
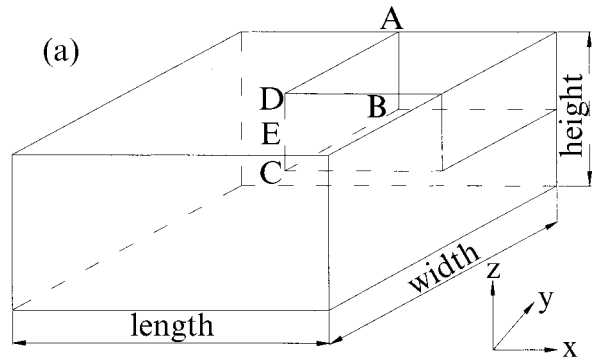
$$f = f^*(f_{ri-1} + f_{i-1})f_{max} \quad \dots \quad (14)$$

where f_{i-1} and f_{ri-1} are, at time of $i-1$, the volume fractions of the new phase and retained austenite respectively. f_{max} is the maximum volume fraction at the temperature of T_i .

The volume fraction of martensitic transformation was calculated by the Koistinen–Marburger equation.²⁰

$$f = 1 - \exp(-\alpha(M_s - t)) \quad \dots \quad (15)$$

where M_s is the starting temperature of martensitic



a geometry; b FEM mesh

2 Geometry diagram and FEM mesh of the large sized block

transformation, T is the temperature, α is a constant depending on the steels, $\alpha=0.021$ for 718 steel.

Properties of the large sized block and quenching processes

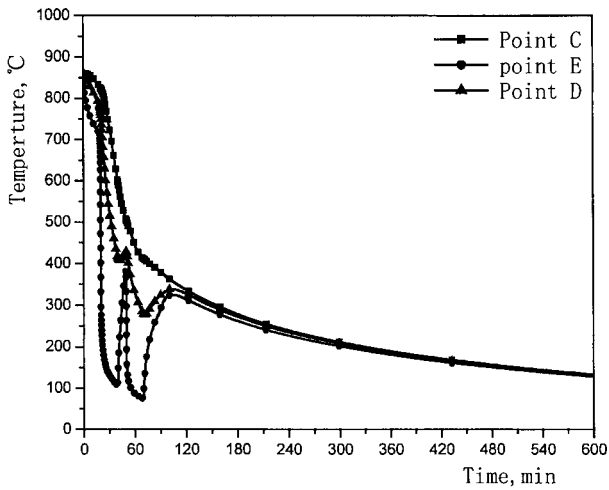
Figure 2a is the shape of the large block. Because of the symmetry, only one eighth of the whole block needs to be simulated and its FEM mesh is shown in Fig. 2b. In order to simulate accurately and reach convergence easily, the bias method is adopted to discretise the block into FEM mesh.

718 steel was developed by ASSAB Company in Sweden by adding approximately 1% nickel to AISI P20 steel (3Cr2Mo). Its chemical composition is shown in Table 1. Before being made into dies, the steel is generally pre-hardened by heat treatment to 280–325HB (29–35HRC) with the largest hardness difference of 3HRC within the same section. The key problem in obtaining uniform hardness without any quenching cracks in large-sized blocks is to design an appropriate quenching process. In traditional quenching with oil as the quenchant, the depth of hardening is thinner and the cost is higher, while there is a higher risk of cracking when water is used as a quenchant. This paper compares the two quenching processes by computer simulation and experimental test. The first investigation is for a combination of pre-cooling, water quenching and self-tempering. The operation sequence is as follows: pre-cooling in air→quenching in the water for a suitable period→self-tempering in air, taking the block out of the water→quenching in the water again for another period→cooling in the air. The second investigation is for

Table 1 Chemical composition of 718 steel, wt-%

C	Si	P	S	Cr	Mn	Ni	Cu	Mo	Fe
0.35	0.40	0.012	0.007	1.75	0.75	1.14	0.11	0.40	Bal.

Published by Maney Publishing (c) IOM Communications Ltd



3 Cooling curves of points along the centre axis (CD) of the block by quenching process I

direct air cooling, that is, first austenitising at temperature as high as 880–930°C, then directly cooling in the air.

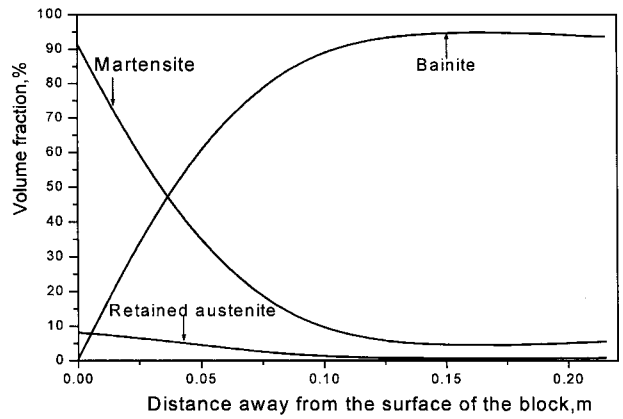
Results and analysis

WATER QUENCHING WITH PRE-COOLING AND SELF-TEMPERING PROCESS

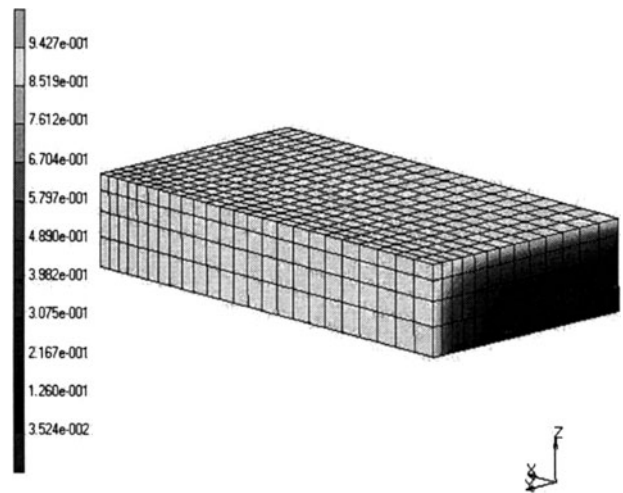
The first quenching process, water quenching with pre-cooling and self-tempering technology, was proposed based on the simulation of a block of 2450 mm × 1300 mm × 430 mm in size, and the results were validated by experiment.

Simulation results show that from the surface to the centre of the large-sized block, martensite and bainite are formed and there is no ferrite or pearlite, which can have a negative effect on the hardness distribution of the whole block (see Fig. 4). Self-tempering between the two quenches in water can be easily identified because raises the surface temperature to about 400°C (Fig. 3). It can effectively decrease the brittleness of the newly formed martensite. In addition, pre-cooling in air before quenching into water can reduce the heat energy of the whole block and the consequent cooling rate of the block surface. Both pre-cooling and self-tempering are helpful to avoid quenching cracks. Therefore the quenching process may meet the requirement of the 718 steel block.

The practical quenching and tempering processes proposed based on simulation are shown in the Fig. 6 to validate the accuracy of the simulation and the feasibility of this quenching process. The experiment on the first quenching process was carried out in Shanghai No. 5 Steel Plant. As shown in Table 2, after heat treatment, the hardness of the whole block is in the range 29–34HRC, with the largest difference being 5HRC. At the surface the hardness is higher than that in the centre because the surface layer microstructure is martensite while that of centre layer



4 Microstructure distributions along the centre axis (CD) by quenching process I



5 Martensite contour of the whole block after quenching process I

is bainite, which can be clearly seen in Fig. 7. Comparing Fig. 7 and Fig. 4, the experimental results are consistent with those of the simulation.

Some quenching cracks can be found at the edges or surfaces of the block, which are related to the martensite formed there, shown in Fig. 5, so in order to meet the strict requirements the quenching process needs to be further improved.

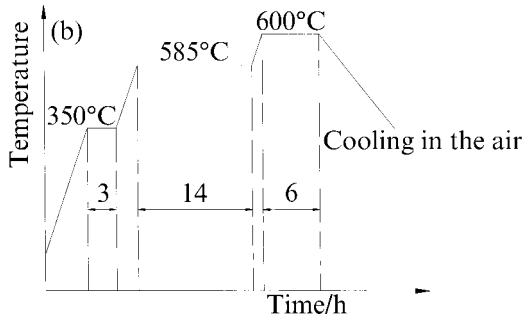
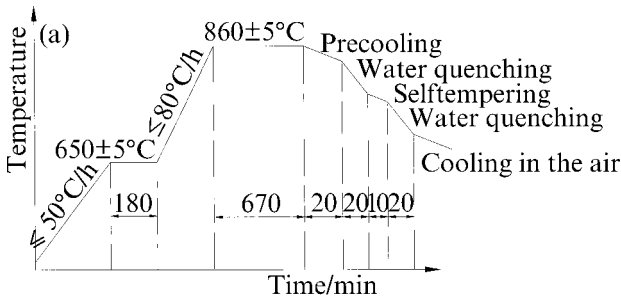
DIRECT AIR-COOLING QUENCHING PROCESS

As seen in Table 2, the hardness uniformity of the block quenched by the first quenching process can not reach the required standard because of different microstructures obtained at the centre and the surface layer. In addition, it was found that there was no ferrite and pearlite transformed in the block because of the higher hardenability (refer to the TTT diagram shown in Fig. 8).

Table 2 Hardness distribution along the height of the block after quenching process I

Distance from the surface, mm	Hardness, HRC	Distance from the surface, mm	Hardness, HRC	Distance from the surface, mm	Hardness, HRC
10	34	130	31.5	250	30.5
30	33	150	31.5	270	30.5
50	33	170	30	290	31
70	32	190	29	310	31
90	32	210	29	330	32
110	31.5	230	30

Published by Maney Publishing (c) IOM Communications Ltd

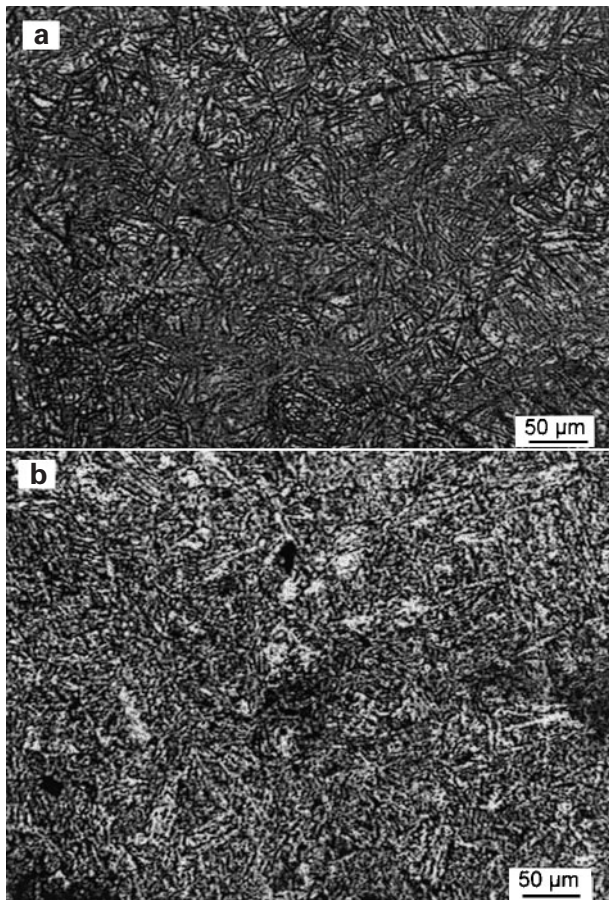


a quenching process I; b tempering process I

6 The flow diagram of quenching and tempering process I

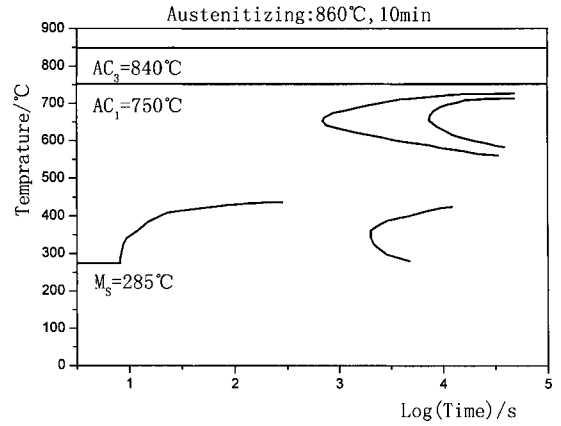
Therefore, a novel quenching process, the direct air-cooling process, was investigated.

The direct air-cooling process was simulated on the block with size of 1100 mm × 1040 mm × 310 mm. From the

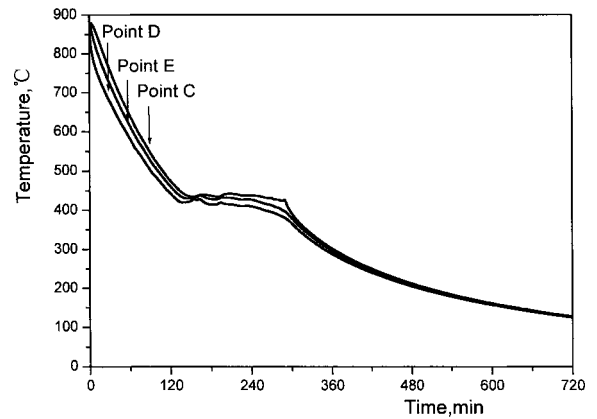


a surface; b centre

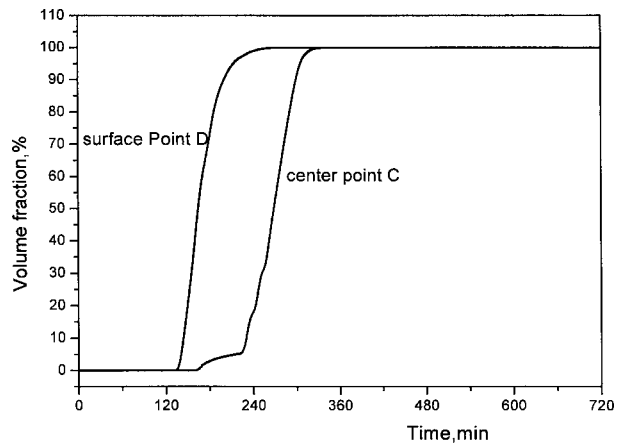
7 Microstructures of the block after treating with the process in Fig. 6



8 TTT diagram of 718 steel used for plastic dies



9 Cooling curves of points along the centre axis (CD) of the block by quenching process II



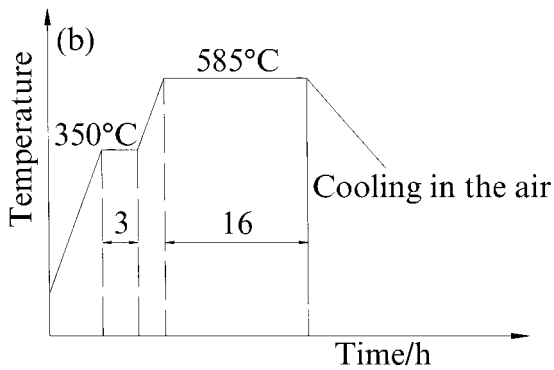
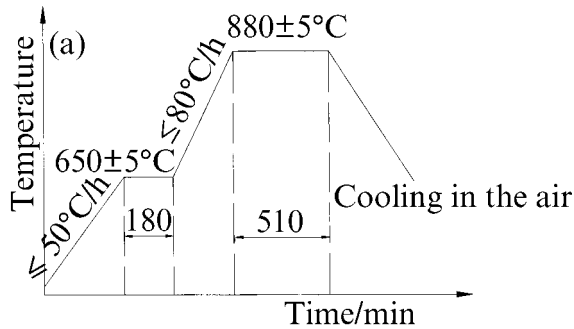
10 Bainite transformation evolution in the block during quenching process II

cooling curves of points at different position on the block, it can be found that the temperature difference is much smaller compared with the first quenching process. As seen from Fig. 9, a temperature flat zone between the 400°C and 450°C can be found, which is caused by release of latent heat of bainite transformation. The simulation phase transformation evolution in Fig. 10 also shows that not only the surface but also the centre of the block transformed into bainite transformation after air-cooling. This can guarantee more uniform hardness distribution. Meanwhile, a small temperature difference between the surface and centre can also effectively avoid quenching cracks.

Published by Maney Publishing (c) IOM Communications Ltd

Table 3 Hardness distribution along the width of the block after quenching process II

Distance from the surface, mm	Hardness, HRC	Distance from the surface, mm	Hardness, HRC	Distance from the surface, mm	Hardness, HRC
10	31.5	150	32.0	330	32.5
30	32.5	170	31.5	350	33.0
50	32.0	190	31.0	370	34.0
70	32.0	210	32.0	390	33.0
90	32.0	270	31.0	410	32.0
110	31.0	290	32.5	430	31.5
130	32.0	310	32.0	450	31.0



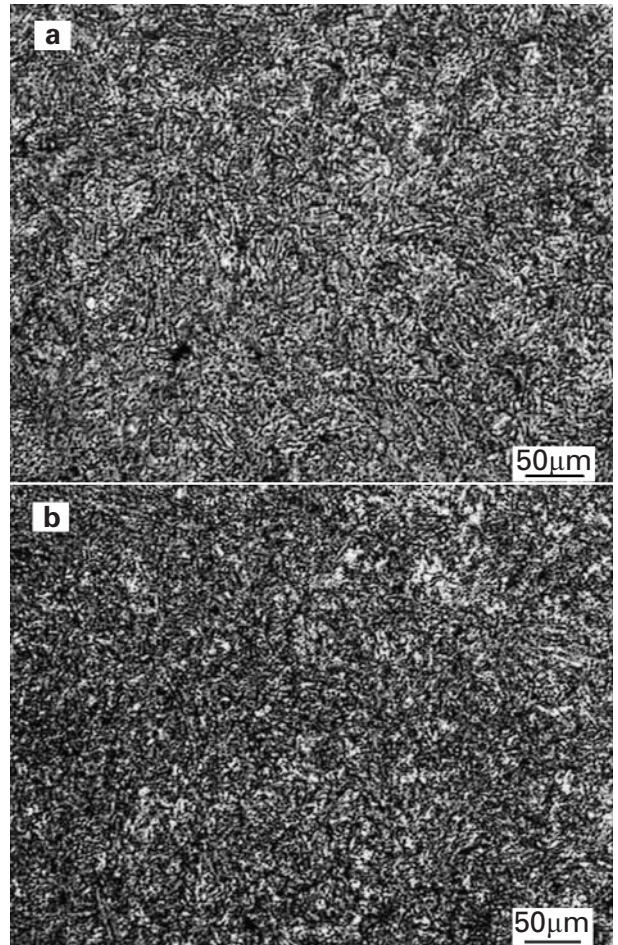
a quenching process II; b tempering process II

11 The flow diagram of quenching and tempering process II

Validation experiments have also been performed as above according to the proposed quenching process shown in Fig. 11. Experiment results in Table 3 shows that the hardness is relatively uniform in the scope of 31–34HRC with the largest hardness difference of 3HRC. The uniformity of hardness distribution lies in the fact that granule bainite is transformed not only at the surface but also in the centre after direct air-cooling (see Fig. 12). Furthermore, there are not any quenching cracks found on the block after heat treatment, so direct air-cooling quenching can completely meet the hardness distribution requirement without risk of cracking.

Conclusion

Through computer simulation and experiment, two quenching processes for large-sized 718 steel blocks used for plastic dies, the water quenching with pre-cooling and self-tempering process and the direct air-cooling process were respectively investigated. In the first quenching process, the hardness of the whole block can be kept in the range 29–34HRC with a maximum hardness difference of 5HRC, but some small quenching cracks can be found at the edges and on the surfaces. In the second quenching process, a more uniform hardness distribution of 31–34HRC with a maximum hardness difference of 3HRC was obtained and



a surface; b centre

12 Microstructures of the block after treating with the process in Fig. 11

no quenching cracks were found, so it is concluded that the direct air-cooling quenching process is more suitable for large-sized 718 steel blocks.

Acknowledgements

The authors wish to thank the Shanghai No. 5 Steel Plant for supporting this work.

References

1. T. INOUE and K. JANAKA: *J. Soc. Mater. Sci. Japan*, 1973, **22**, 218–223.
2. S. DENIS and P. ARCHAMBAULT: Proc. 3rd Int. Conf. on 'Quenching and control of distortion', Prague, Czech Republic, March 1999, 263–266.

3. B. BUCHMAYR and J. S. KIRKALDY: *J. Heat Treatment*, 1990, **8**, 127–136.
4. J. S. PAN, M. J. HU, D. TIAN and D. RUAN: *Heating Technol.*, 1998, **1**, 1–4.
5. X. CHEN: *Adv. Mater. Process.*, 1997, **152**, 44w–44y.
6. Z. Y. XU: 'The principle of phase transformation', 1st edn; 1988, Beijing, China, Science Press.
7. T. RETI, Z. FRIED and I. FELDE: Proc. 3rd Int. Conf. on 'Quenching and control of distortion', Prague, Czech Republic, March 1999, 157–172.
8. T. T. PHAM and E. B. HAWBOLT: *Metall. Mater. Trans. A*, 1995, **26A**, 1993–1999.
9. F. M. B. FERNANDES, S. DENIS and A. SIMON: *Mater. Sci. Technol.*, 1985, **1**, 838–844.
10. Z. LIU, Z. J. WU, J. Z. WU and Y. ZHANG: 'The numerical simulation on heat treatment process', 1st edn, 119–158; 1996, Beijing, China, Science Press.
11. Z. C. ZHU and Z. Y. XU: *Trans. Metal Heat Treatment*, 1988, **9**, (2), 45.
12. A. J. BAKER, P. D. MANHARDT and J. A. ORZECOWSKI: Proc. 2nd Int. Conf. on 'Quenching and control of distortion', ASM International, Materials Park, OH, 1996, 283–296.
13. J. S. PAN and M. J. HU: *Heat Treatment Metals*, 1998, **12**, 26–31.
14. P. R. WOODARD, S. CHANDRASEKAR and H. T. Y. YANG: *Metall. Mater. Transform. B*, 1999, **30B**, 815–822.
15. X. YAO: 'The application of computer simulation on the quenching of large-sized mould blocks and bearing steel', 28; 2003, Dissertation, Shanghai Jiao Tong University.
16. A. M. S. HAMOUDA, S. SULAIMAN and C. K. LAU: *J. Mater. Process. Technol.*, 2001, **119**, 354–360.
17. H. P. HOUGARDY and K. YAMAZAKI: *Steel Res.*, 1986, **57**, 466–471.
18. P. K. AGARWAL and J. K. BRIMACOMBE: *Metall. Trans. B*, 1981, **12B**, 121–133.
19. A. W. JOHNSON and R. F. MEHL: *Trans. AIME*, 1939, **135**, 416–458.
20. D. F. KOISTINEN and R. E. MARBURGER: *Acta Metall.*, 1959, **7**, 50–60.